Naval Research Laboratory
Washington, DC 20375-5320

NRL/MR/6680--94-7634

Surface Damage Effects Generated by A Fast-Pulse Laser Beam

P.G. BURKHALTER
J.H. KONNERT

Dynamics of Solids Branch
Condensed Matter & Radiation Science Division

E.F. GABL

Clark-MXR, Inc.
Dexter, MI 48130

December 6, 1994

REPORT DOCUMENTATION PAGE

Form Approved
OMB No. 0704-0188

1. AGENCY USE ONLY (*Leave Blank*)	2. REPORT DATE	3. REPORT TYPE AND DATES COVERED
	December 6, 1994	

4. TITLE AND SUBTITLE

Surface Damage Effects Generated by a Fast-Pulse Laser Beam

5. FUNDING NUMBERS

PE -66-2848-05

6. AUTHOR(S)

P.G. Burkhalter, J.H. Konnert and E.F. Gabl*

7. PERFORMING ORGANIZATION NAME(S) AND ADDRESS(ES)

Naval Research Laboratory
Washington, DC 20375-5320

8. PERFORMING ORGANIZATION REPORT NUMBER

NRL/MR/6680--94-7634

9. SPONSORING/MONITORING AGENCY NAME(S) AND ADDRESS(ES)

Office of Naval Research
800 North Quincy Street, BCT #1
Arlington, VA 22217-5660

10. SPONSORING/MONITORING AGENCY REPORT NUMBER

11. SUPPLEMENTARY NOTES

*Clark-MXR, Inc., Dexter, MI 48130

12a. DISTRIBUTION/AVAILABILITY STATEMENT

Approved for public release; distribution unlimited.

12b. DISTRIBUTION CODE

13. ABSTRACT (*Maximum 200 words*)

A fast-pulse laser was used to induce damage on the surface of a polished silicon wafer. Effects of focused-laser heating at threshold for damage were examined with high-resolution imaging microscopes. The extent and characteristics of various ripple structure were measured with an atomic force microscope.

14. SUBJECT TERMS

surface damage
fast-pulse laser

15. NUMBER OF PAGES

15

16. PRICE CODE

17. SECURITY CLASSIFICATION OF REPORT	18. SECURITY CLASSIFICATION OF THIS PAGE	19. SECURITY CLASSIFICATION OF ABSTRACT	20. LIMITATION OF ABSTRACT
UNCLASSIFIED	UNCLASSIFIED	UNCLASSIFIED	UL

NSN 7540-01-280-5500

Standard Form 298 (Rev. 2-89)
Prescribed by ANSI Std 239-18
298-102

SURFACE DAMAGE EFFECTS GENERATED BY A FAST-PULSE LASER BEAM

INTRODUCTION

This work involved the interaction of a focused-laser beam with crystalline silicon to study the induced surface damage. A fast-pulse, laser (155 femtosec) operating at a kilohertz pulse rate was used to induce surface damage. With a high-resolution microscopes, one can examine the surface morphology of this threshold laser damage. The laser damage was found to be in the form of ripple patterns. The damage patterns were obtained with a few millijoules of unpolarized, multi-shot, focused-laser-beam intensity. The laser beam was focused at nearly normal- incidence onto single- crystal silicon (100) wafers. The ripple effect has been identified[1] as alternating areas of amorphous and crystalline silicon resulting from heating by thermal gradients. Previous studies to measure threshold damage with lasers operating in the picosec time regime. Laser-induced surface damage studies in silicon with 20 ps pulses to generate ring structure damage used unpolarized laser light[2].

Circular damage areas were obtained[3] using slightly longer pulses (46 ps) at 1.0 μm laser illumination. Threshold values varied from 0.6 to 3 J/cm^2 for picosecond pulses. Circular areas of surface damage using unpolarized laser light and evidence of evaporation and recrystallization were seen. At the shortest pulse duration (4 ps) the laser damage was seen as a circular area with a ripple surface. This is in contrast to linear damage areas resulting from laser-induced periodic surface structure (LIPSS) patterns as observed with linearly-polarized light[4,5].

The laser in our work fired with a short pulse and was well focused to yield high irradiance. This generated craters of about 10 um diameter with well-defined, sharp sides. At the low laser energies, a large circumference propagation ring was formed with a separation of about 150 μm from the central crater.

Manuscript approved October 24, 1994.

EXPERIMENTAL

The highly-focused fast-pulse (155 fsec) laser of 0.8 μm light was used to generate damage in the surface of polished silicon at various laser energies. The laser energy on target was varied using optical filters from a few μJ to about one mJ on target. A series of shots was taken with different filters for determining the threshold for surface damage as the laser energy and pulse duration were varied.

The surface morphology was examined with high-resolution SEM and AFM microscopes. There existed microscopic evidence for melting, evaporation, and ablation of particles.

The laser energy was varied in a series of shots. The laser spots were examined with a light microscope to correlate the effect with the laser energy. At a low energy of 0.3 μJ/pulse, no surface damage was visible with 5 seconds of firing at 1 kHz. At an energy of 70 μJ/pulse, the central crater plus a faint outer ring were formed in a few thousand shots. At high-irradiance with no absorption filter, a 0.43 mJ/pulse produced multiple ring structure in one-half second of firing.

RESULTS

At an irradiance of $3.5*10^{14}$ to $2*10^{15}$ W/cm^2 catastrophic damage was generated in the form of a deep crater at the center of the focal region. The surface damage occurred in a central spot of 10-15 μm in diameter. At a distance from the central focal region was a damage region in the shape of a partial ring or annulus. In shots of lower irradiance, an asymmetric circumferential ring about 150 μm from the central focus was formed. This semi-circular area probably results from a portion of reflected light. The laser was operated at tight-focus and a sequence of shots were fired to collect laser damage regions at different energy levels and time durations. The laser energy was varied using optical filters. At higher energy (less filter absorption) and longer time durations (several seconds), the laser focal spots were visible on the surface of the polished silicon wafer. Examination under a microscope revealed an asymmetric or semi-circular ring pattern surrounding a catastrophic damage area at the focal center. Figure 1 are SEM images of the laser damage region collected at high irradiance. In image a), a deep indentation can be seen forming at the center of the focal spot region. Structural differences appear in the outermost rings compared with the regularities seen in the dozen or so inner rings. The origin of the asymmetry of the ring pattern is unknown but probably results from the alignment of the focusing lens. A higher-resolution view in b) shows the consistency of the uniform ring pattern and the large, radial striations that comprise the ring damage. Close-up views in c) of the outer ring shows an enhancement of molten-looking tubular structure. Ripples are seen in the structure of the outermost zone (Fig.1d). In addition to the ripple regularities there exists a finer detail appearing as a dotted damage structure beyond the ripples.

Various laser damage regions collected at lower irradiance were examined. SEM images showing the laser damage pattern at lower irradiance are presented in Fig.2. The patterns consist of a central region having the appearance of a deep central crater with laser damage in the form of a single peripheral ring located a distance from the crater. These images were scanned with the specimen rotated 90 to the images at high irradiance. A higher magnification SEM image seen in b) shows a molten tubular structure with burst holes throughout the mid-section of the peripheral ring and a mottled dot appearance about 2.5 μm wide on the outermost side of the ring. The blow-up of the central focal region has the appearance of deep tubular areas of molten silicon sections with burst holes and ripple surfaces forming the sides. Image d) is a close-up view of the parallel tubular ripple structure that looks similar to the mid-section outer zone of the peripheral ring. There also exists a faint ripple structure that extends as much as 5 μm beyond the coarse tubular structure on the surface of the polished silicon surface. The structure of the outer ring in this low-irradiance shot (produced with the least energy to observe laser damage) was scanned with the Scanning Electron Microscope.

Figure 3a shows the SEM close-up image of the mid-section of the peripheral ring. Large striations with ~0.8 μm spacings and widths are seen at the center of the mid-section. There exists regularities in the form of dots that could connect and extend the radial structural formation. Also, striations orthogonal to the radial structure are observed along the circumference in the mid-section pattern. The outer regions appear as semi-ordered molten dots on both sides of the peripheral ring. These dots appear to coalesce into the two ripple patterns. Figure 3b shows the structure at the lower end of the peripheral ring. There are several apparent features. An overall large ripple pattern exists with 1 μm spacings and 1 μm width looking like mountain-range striations. There are molten islands or dots are distributed randomly at the tip of the damaged zone. The outside of the ring has a faint ripple pattern with spacings of 0.20 μm as seen extending away from the larger damage region similar to that extending from the central crater in Fig. 2d.

Surface measurements on a submicron level can be from images obtained by scanning in the Atomic Force Microscope. In addition to observing the surface morphology, one can measure the surface roughness of selected areas in the collected images. Linear scans across the AFM images can be used to measure surface feature such as the spacings and peak- to- valley ratios of ripples. The AFM image in Fig. 4a was collected on the inner edge of the mid-section of the peripheral ring over a 10 μm^2 scan. The large striations in the center are about 1 μm wide and have about 1 μm spacings. The circumferential parallel lines have about 0.5 μm separation. The spacings between the rows of bright dots were determined from transverse scans shown in Figs. 4b and 4c. The spectral period for both of the dot patterns was found to be 0.24 μm. The spatial frequency was determined to be 0.22 μm from the 2-D Fourier transform of the spectral density plot in Fig. 4c. Another AFM scan of an outside area of the ring structure gave a spacings of 0.21 μm for the separation of the lines and spacings of rows between dots in the ripple pattern. The dot pattern apparent in 4b and 4c forms a structure with short range 2-D periodicity. This is further emphasized b 4d, which is the 2 dimensional Fourier transformation of 4c. Each sharp maxima in 4d is associated with a periodic set of parallel lines in 4c. Therefore, the dots of molten silicon areas appear to coalesce into the fine ripple structure.

An AFM image of the middle portion of the peripheral mid-section is shown in Fig. 5. This area is similar to the mid-section image of the SEM scan shown in Fig. 3a. The spatial frequency of the large striations in the center was found to be 0.9 μm from the orthogonal scan in Fig. 5b. The spacing of the ripple structure on the lower edge of the damage zone is 0.5 μm. The faint ripple structure extending beyond the damage zone has a spacing of 0.21 μm.

The AFM was utilized to examine the surface structure at the lower tip of the peripheral ring. Figure 6a shows the large ripple features of the area that appeared also in the SEM image shown in Fig. 3b. A topographical view of the ripple structure is seen in Fig. 6b. A zoomed view of the ripples is presented in Fig. 6c showing the parallel structure of the ripples and the transverse scan Fig. 6d gives the separation distances across the ripple structure found from the transverse scan. From these images we learn that the ripples are parallel with nearly uniform spacings of $\sim 1/2$ μm and widths of $\sim 1/2$ μm. Beyond the ripples the laser heating generates an assembly of random molten spots.

DISCUSSION

The high-irradiance short-pulse laser induced surface damage has several distinct features. In this work the tight-focused laser spot produced a deep crater with side walls formed of molten silicon as evidenced from the microscopic examination showed an appearance like melting, edge bursting and evaporation. The question of debris ejection from the catastrophic crater formation was considered. At a distance of a few hundred microns outside the laser damage peripheral zone the surface roughness was measured and found to be 6.4 Å over a 1 μm^2 area. Some debris particles were found in the intermediate area between the crater and the peripheral ring. Typical roughness values of 20 Å over 1 μm^2 and 60 Å over 10 μm^2 areas were determined indicating some slight laser heating in this area. Large debris particles were not found as was the situation case in other work using a long-pulse 1/4 μm excimer laser[6] where numerous debris particles were found near the laser focal region and areas within several hundred microns from the edge of the focal spot.

CONCLUSIONS

The observations with the AFM show coalescing of molten particles forming into ripple structure. The separation of the particles and the alignment into apparent rows with 0.21 μm spacings that extend from the edge of the tubular regions. There also are found to be parallel structure formed with larger 0.5 μm spacings. The width of the outer single peripheral zone was 10-12 μm. The multiple zones had widths of about 15 μm. Distinctive surface damage features in this study are the multiple rings seen in the higher energy shots.

REFERENCES

1. P. L. Liu, R. Yen, N. Bloembergen, and R. T. Hodgson, Appl. Phys. Lett. 34(12),864 (1979).

2. J. M. Liu, R, Yen, H. Kurz, and N. Bloembergen, Appl. Phys. Lett. 39 (9),755 (1981).

3. I. W. Boyd, S. C. Mjoss, T. F. Boggess, and A. L. Smirl, Appl. Phys. Lett. 45(1), 80 (1984).

4. H. M. van Driel, J. E. Sipe, J. F. Young, Phys. Rev. Lett. 49(26), 1955 (1982).

5. J. E. Sipe, J. F. Young, J. S. Preston, and H. M. van Driel, Phys. Rev. B 27(2), I. Theory, 1141, II. Experiments, 1155 (1983).

6. P. G. Burkhalter, R. C. Y. Auyeung, D. B. Chrisey, and J. H. Konnert (to be published).

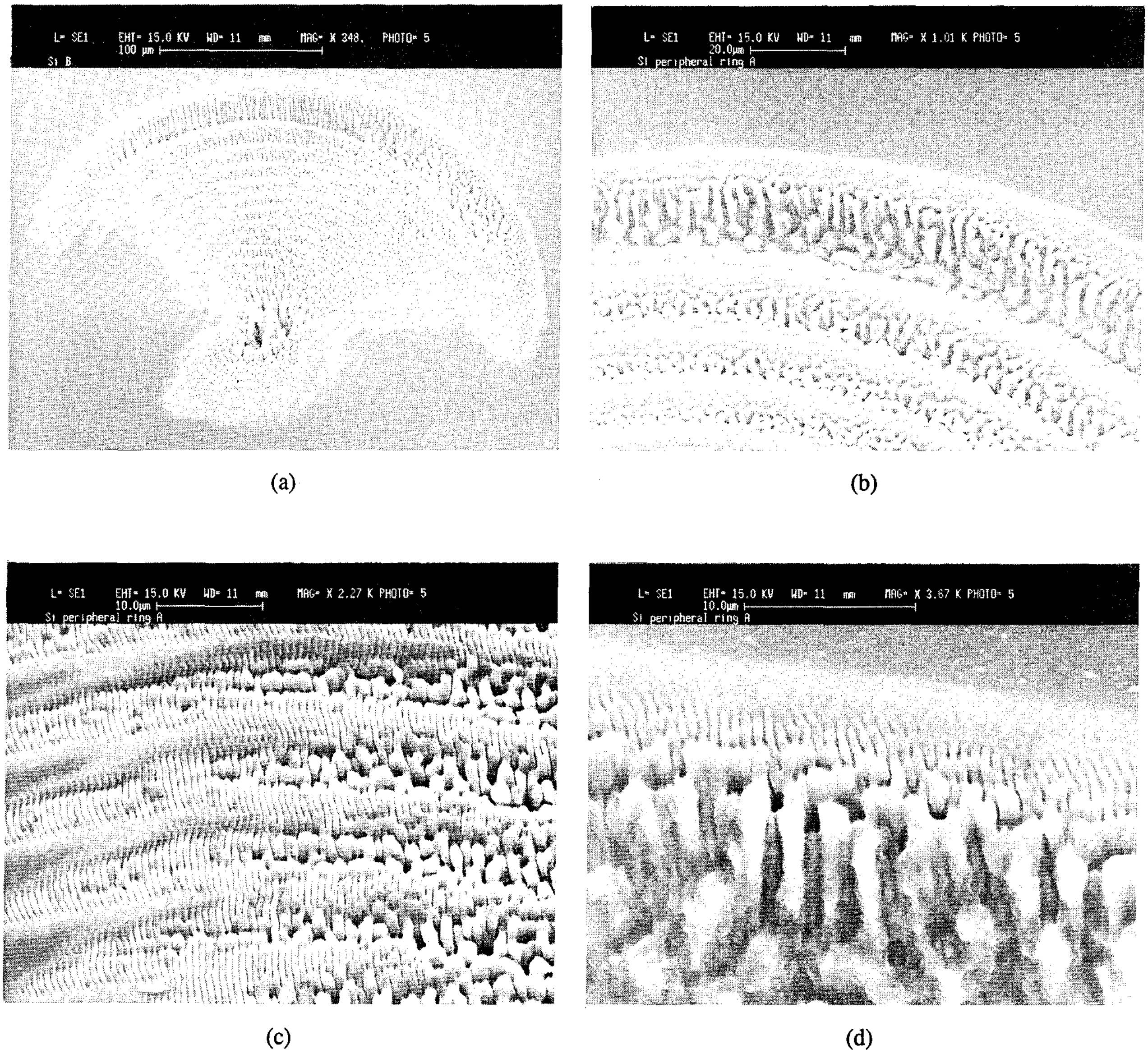

Fig. 1. SEM images of high-irradiance, fast-pulse focal area showing a) the entire laser damage region, b) high-magnification view of multiple ring structure, c) and d) close-up details of outer ring structure.

Surface crater Focal area

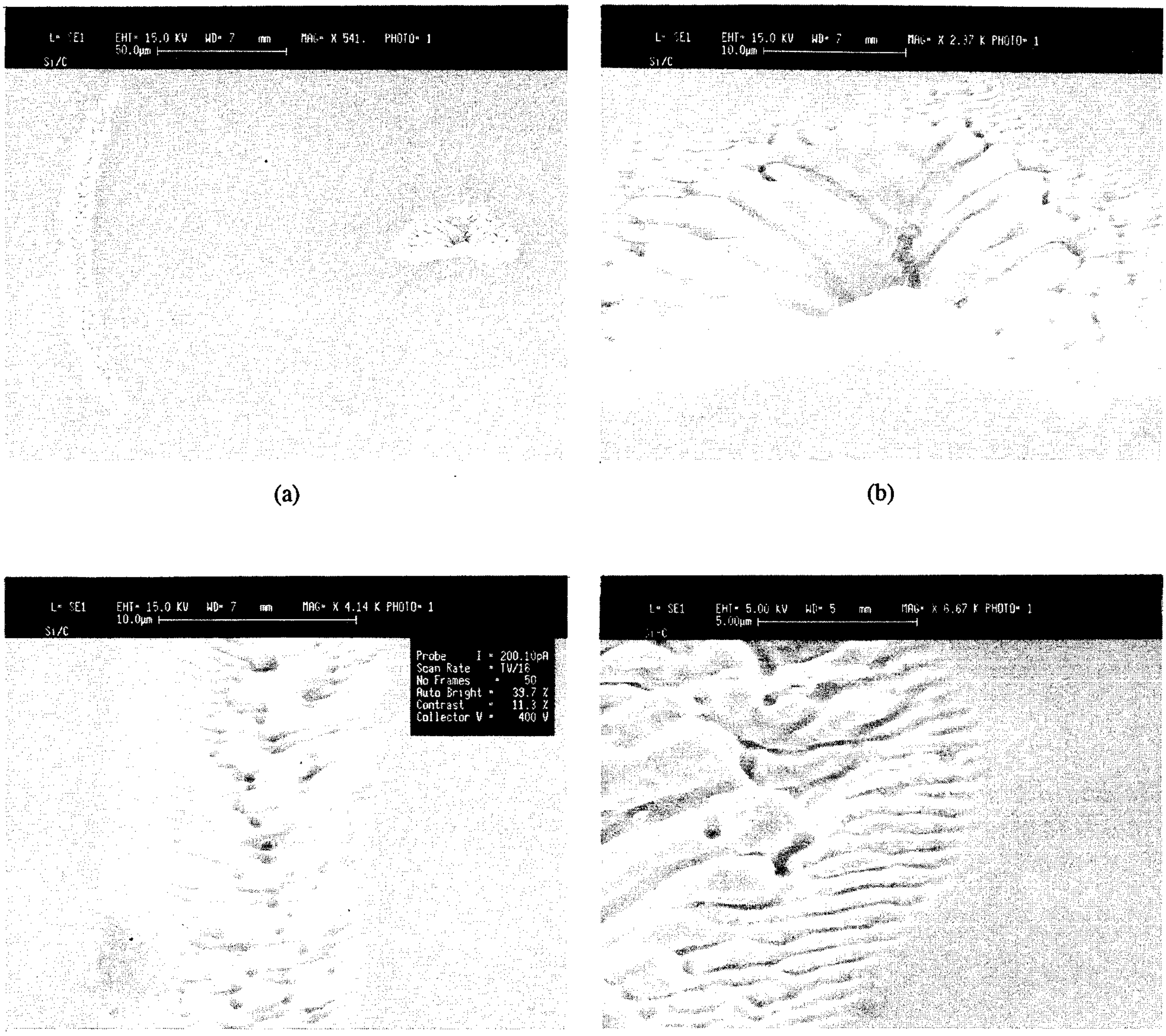

(a) (b) (c) (d)

Fig. 2. SEM images of low-irradiance laser focal area a) entire laser damage region, b) zoomed view of the mid-section of the peripheral ring, c) close-up view of the central focal area, and d) edge of focal spot showing ripples extending into the smooth surface area beyond the crater.

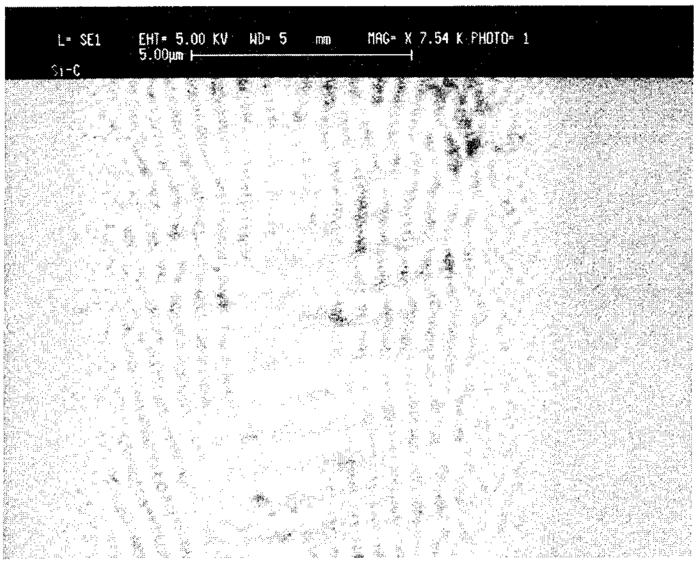

(a)

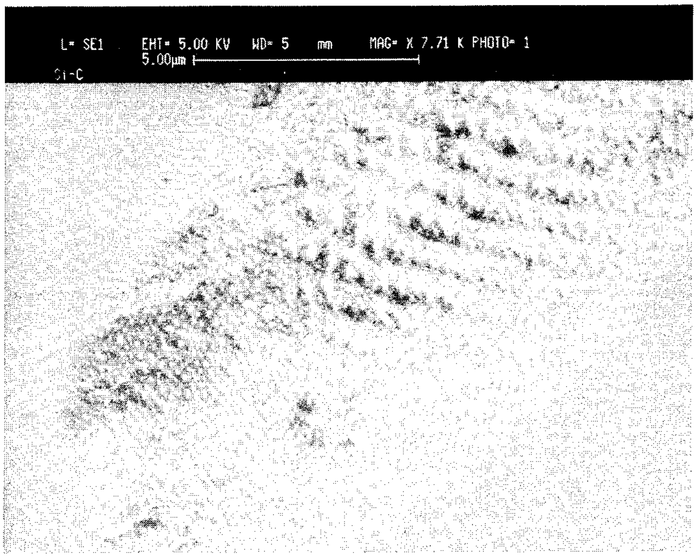

(b)

Fig. 3. SEM images of peripheral zone at near threshold damage: a) mid-section region and b) tip of peripheral zone.

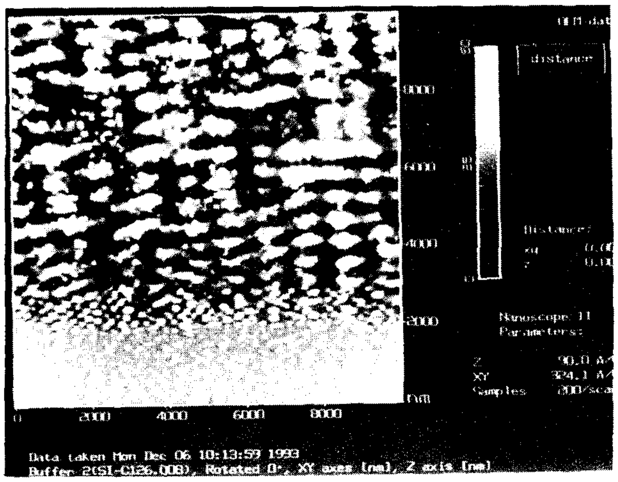

(a)

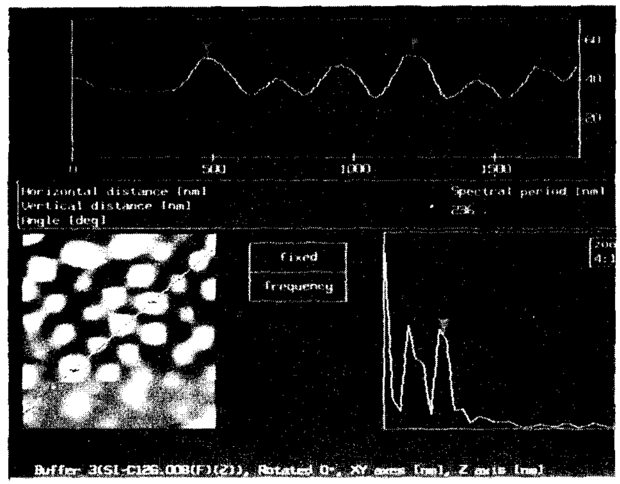

(b)

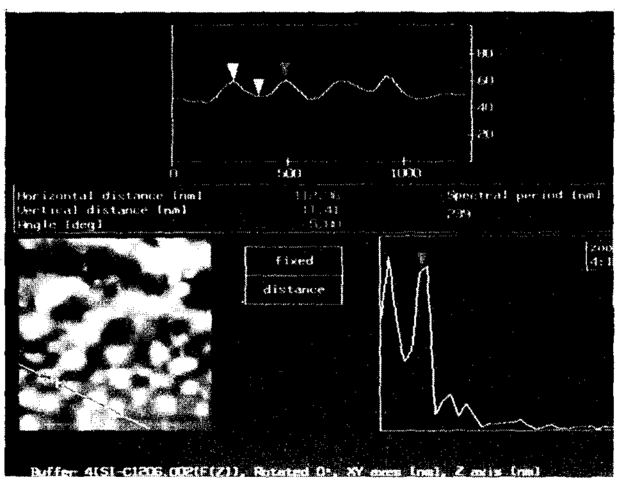

(c)

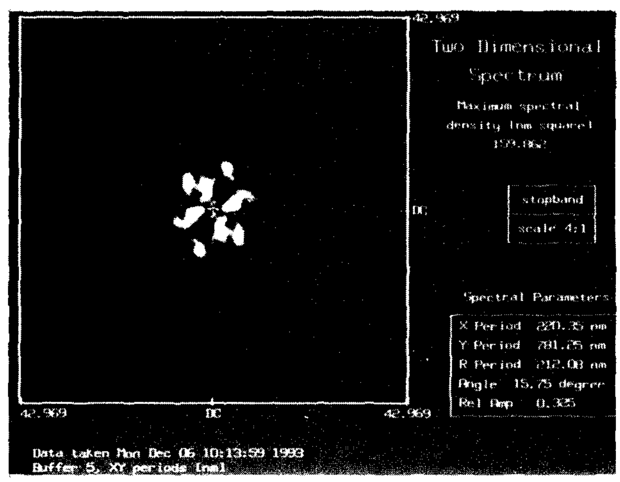

(d)

Fig. 4. AFM image in the peripheral zone, showing a) image of the mid-section, b) transverse scan of mid-line, c) scan of large ripples, and d) scan of fine ripple structure.

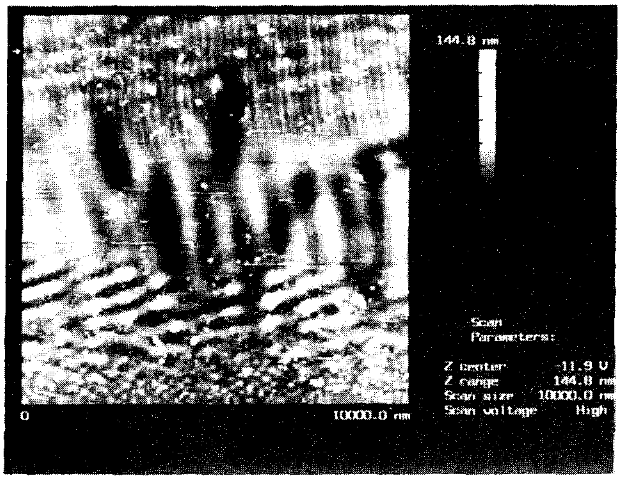

(a)

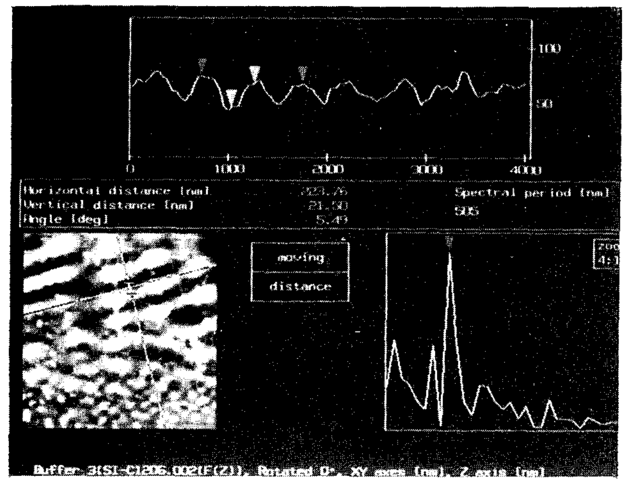

(b)

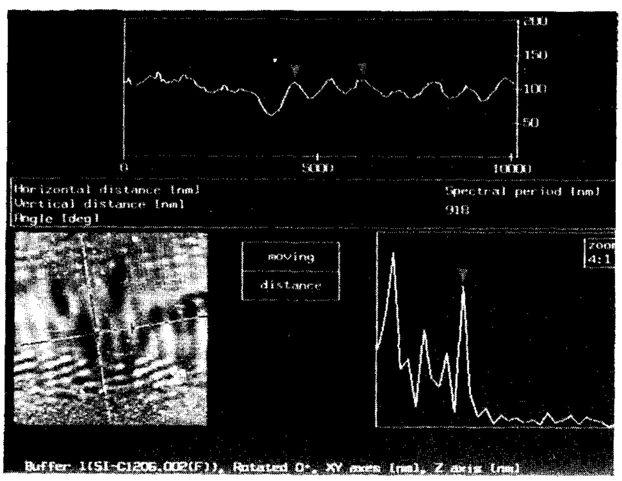

(c)

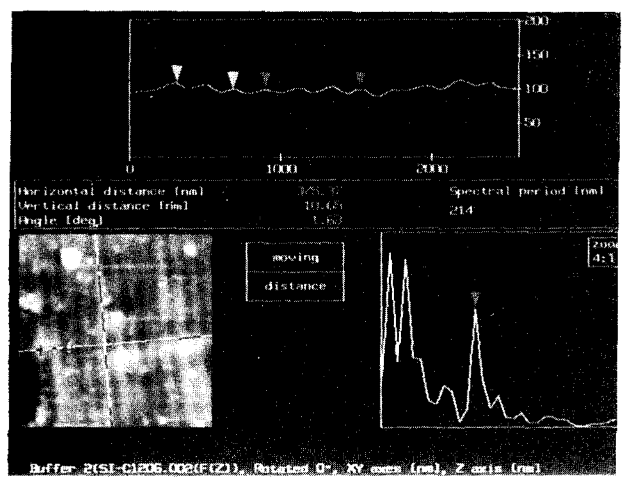

(d)

Fig. 5. AFM image of mid-section edge structure in the peripheral damage zone, showing a) inner region image, b) transverse of molten edge structure of damaged region, c) orthogonal transverse of edge structure, and d) Fourier spatial frequency plots.

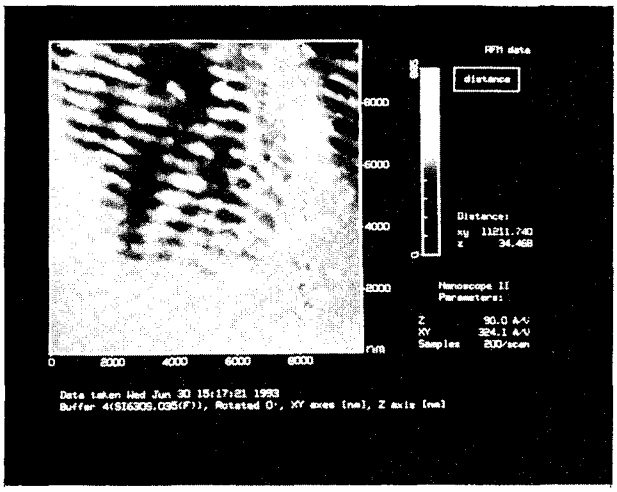

(a)

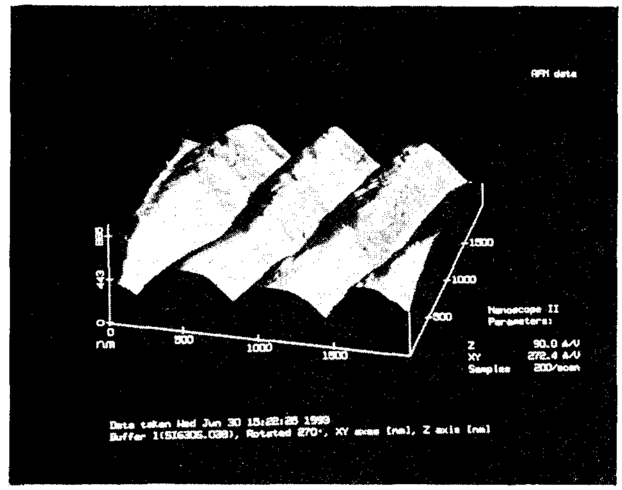

(b)

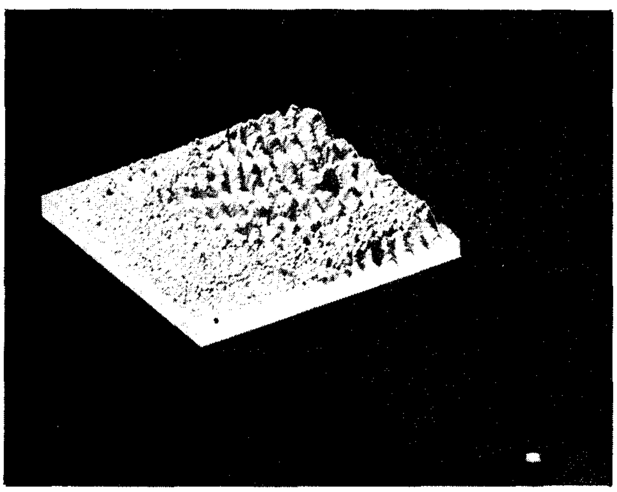

(c)

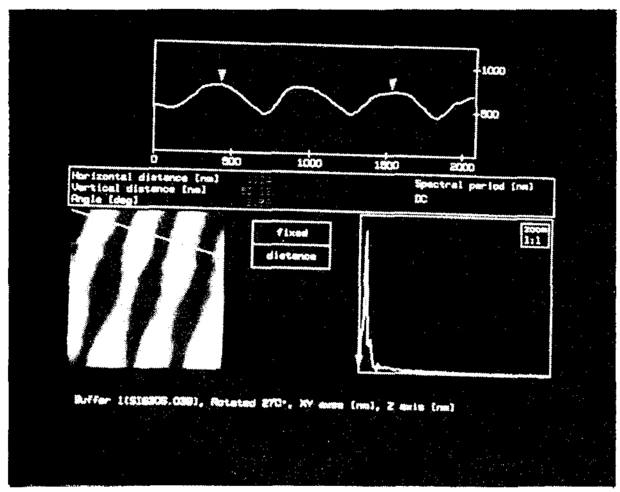

(d)

Fig. 6. AFM images showing, a) the ripple structure, b) topographical view of the tip region of the peripheral zone, c) zoomed view of the ripple structure, and d) transverse scan of the pattern.